Design of Micromechanical Bubble-Jet Devices

Bernhard Hochwind
Technische Universität München, München, Germany

Introduction

The great variety of micromechanical manufacturing processes, particularly anisotropic etching of silicon, provides the opportunity for a wide range of geometries for thermal ink-jet devices. In addition to the capabilities of processes like microlithography, etching of silicon allows the manufacturing of structures in the micrometer range and of special geometries like thin membranes.

For the design of a micromechanical bubble-jet system we need simulation capabilities. Our program includes simulation of heat conduction, of thermodynamics of the vapor bubble, of mechanisms of ink flow and FEM-Simulation of membranes.

By predicting the behaviour of a bubble-jet device our program helps to find the best way to exploit the capabilities of the micromechanical manufacturing technology.

Components of the Simulation Program

The program describes the significant features of a bubble-jet device:

- heat conduction from the heater to the ink and to the vapor bubble;
- detection of nucleation time;
- thermodynamics of the vapor bubble;
- ink flow through nozzle and throttle;
- a simple model for drop formation;
- damping and crosstalk by elasticity of the structures;
- compressibility of the ink.

The listed components are not simulated separately, but in interaction with each other. The following diagram shows the communication between the simulation subroutines by the time-dependent states temperature T(t), pressure p(t) and volume V(t).

In addition to simulating a given structure, the program can also compute the set of input parameters, such as dimensions of nozzle and throttle, thickness of layers or heater current in order to optimize some output parameters, such as drop mass, drop velocity or refill time.

Originally published in *Proc. of IS&T's Ninth International Congress on Advances in Non-Impact Printing Technologies*, October 4-8, 1993, Yokohama, Japan.

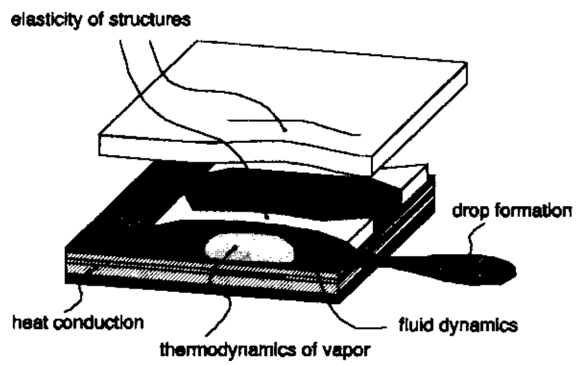

Figure 1. All the essential features of a bubble-jet device are simulated by the program described in this paper

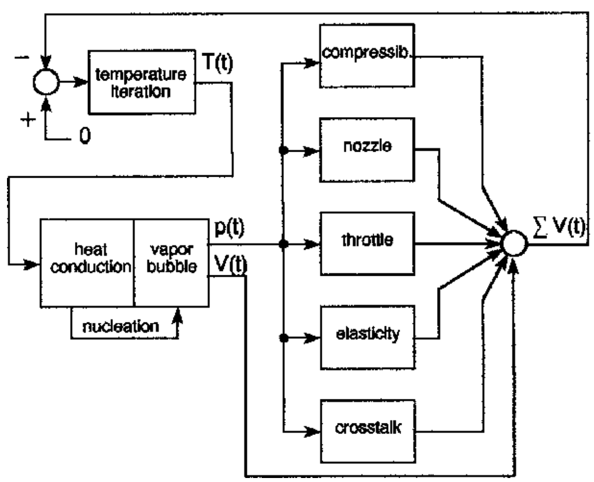

Figure 2. Communication between simulation components

Some components use a reduced model in order to limit the simulation time, especially during optimization. The simulation time for a typical 300dpi bubble-jet requires about 5 to 10 minutes of calculation time on a PC 486-50 and multidimensional optimizations for desired output datas become feasible.

Description of the Simulation Routines

Heat Conduction

Heat conduction in a given layout is simulated in two dimensions. Three-dimensional simulation is not supported because with its high calculation expense it obstructs the finding of a result in an acceptable amount of time and in most cases the heater geometry gives no requirement for it anyway.

The simulation of the vapor-bubble is closely linked to heat conduction, in the sense that its heat exchange is considered in the equations of heat conduction.

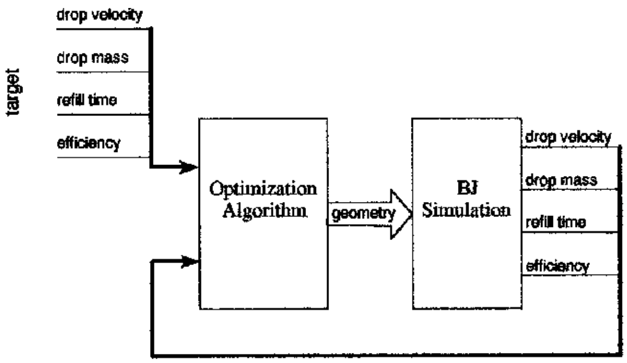

Figure 3. Optimization framework for bubble-jet simulation

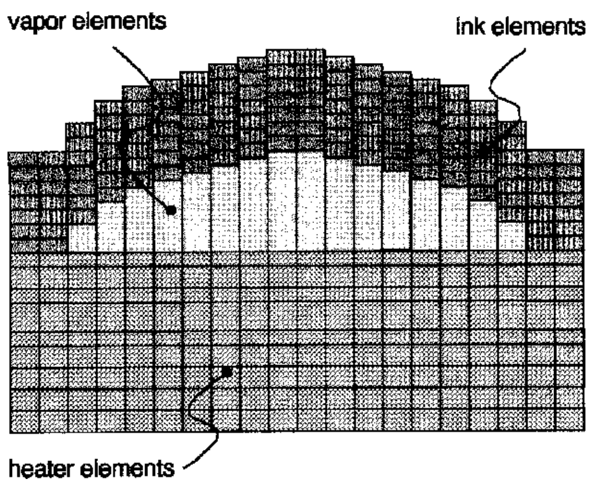

Figure 4. Finite elements for the simulation of heat conduction and of the vapor bubble

Detection of Nucleation Time

The heat conduction segment of the program contains an empirical criterion, derived by measurements on several samples, for the detection of nucleation1. According to the criterion, which analyzes the temperature T and the local temperature gradient $\partial T / \partial s$ on the boundary between heater and ink, nucleation starts when somewhere on the boundary the condition

$$\frac{T}{230°C + 1.6 \cdot 10^{-7} m \cdot \partial T / \partial s} = 1$$

is satisfied.

Thermodynamic Effects in the Vapor Bubble

Thermal-mechanical energy conversion in the vapor bubble is simulated with a one-dimensional finite volumina model[2] linked to the heat conduction subroutine. Each ink element (index i) with borders on the heater surface is assigned a thermically coupled vapor element (heat flow $\dot{Q}$) with a variable volume which is in mechanical interaction (power $\dot{L}$) with the ink flow model as described by:

$$\dot{U} = \dot{Q} + \dot{L}$$

The vaporization and condensation can be calculated adopting saturated vapor by the gradient of the intrinsic energy $\dot{U}$.

The following flow chart sketches the algorithm used in this routine. The temperature T of all vapor elements, which is the single variable of state of saturated vapor is iterated in reciprocal action with heat conduction and the response of mechanical system.

- Calculate density $\rho(t_n)$, pressure $p(t_n)$, intrinsic energy $U(t_n)$ by temperature $T(t_n)$ at time t_n before time step
- Iteration of temperature $T(t_{n+1})$ after time step; whence (*vapor volume* $\Sigma Vi(t_{n+1}) \neq$ *flow volume* $V_f(t_{n+1})$)
  - Calculate $\rho(t_{n+1})$, $p(t_{n+1})$, $U(t_{n+1})$ at temp $T(t_{n+1})$ for each vapor element (i)
    - Calculate heat exchange with environment $Q_i(t_n \rightarrow t_{n+1})$ during transition $t_n \rightarrow t_{n+1}$
    - Calculate vapor volume $V_i(t_{n+1})$ as a function of $V_i(t_n)$, $Q_i(t_n \rightarrow t_{n+1})$, $\rho(t_n)$, $\rho(tn+1)$, $U(tn)$ and $U(tn+1)$
  - Calculate flow volume $V_f(t_{n+1})$ of $p(t_n)$ and $p(t_{n+1})$

The next diagram shows a cross-section of a simulated vapor bubble at a particular time:

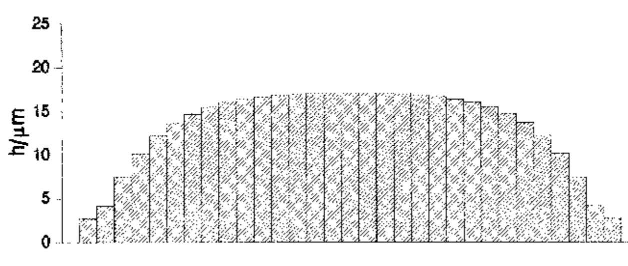

Figure 5. The program accurately computes the shape of a vapor bubble

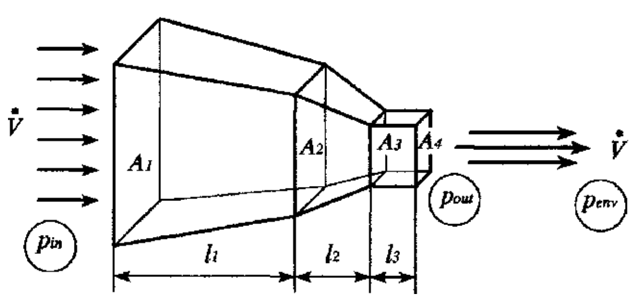

Figure 6. Zones of flow to nozzle and throttle represented in the model

Ink Flow Through Nozzle and Throttle

Zones of flow from the vapor bubble to the nozzle opening and to the ink reservoir are simulated as truncated pyramids through which the ink flows. Laminar pipe flow is adopted for the transient calculation[3].

The following equation is used for the calculation of the pressure gradient between the vapor bubble (pin) and the reservoir/ nozzle (pout)

$$p_{out} - p_{in} = \frac{\rho}{2}\left(\frac{1}{A_1^2} - \frac{1}{A_n^2}\right) \cdot \dot{V}^2 + \sum_{i=1}^{n}\left(8\eta\int_0^{l_i}\frac{d1}{A(1)\cdot R^2(1)} \cdot \dot{V} + \rho\int_0^{l_i}\frac{d1}{A(1)} \cdot \ddot{V}\right)$$

where: ρ is the density;
η is the dynamic viscosity;
R(1) is the equivalent radius of the area A(l).

The model contains terms for acceleration (1st term), friction (2nd term) and non-stationary condition (3rd term). The throttle outlet pressure (pout) is calculated from the reservoir pressure (Penv) according to:

$$p_{out} \approx p_{env} + \frac{\rho}{2A_n^2}\dot{V}^2$$

More complex geometries must be simplified. A commercial fluid dynamic program can be used to find a simple equivalent geometry with comparable characteristics.

Drop Formation

The formation of drops and its effects on the ink flow due to meniscus pressure is described with a simplified model that captures the different phases of the process, namely:

- first phase of drop formation: spherical meniscus;
- second phase of drop formation: cylindrical drop section with adopted constant diameter;
- drop tear off at flow speed = zero;
- refill: spherical meniscus.

Mechanical Properties of the Design/Damping

The design of micromechanical manufactured bubble-jet devices may be based on thin membranes which originate either from anisotropic etching with a corresponding mask or from a barrier which stops the etching process. These elastic structures can be located between adjacent channels, where they cause crosstalk, or between channel and environment, where they cause damping. Both possible locations of structures are considered in the program, although in a simplified manner. Not the entire structures are simulated, but only the features like fundamental resonant frequency, elasticity and damping. These characteristics are extracted from the impulse response of the structure, which is computed, in advance, if an analytic solution is not possible in consequence of complex geometries or gripping. A comparison between detailed simulation of a usual shaped membrane with the reduced model has shown that the volume deflections are differing only about 1%.

Compressibility of ink is modeled as a single outlet of ink without dissipation. This means that the calculation of the vapor bubble collapse can not provide good peak pressure values because acoustical effects are not considered, but this is not important for our simulation.

Application

The simulation program can be used in the design phase of a new bubble-jet device because it can provide early answers to many important questions, related to thermal and mechanical behavior of the device:

Item 1: Heat Conduction

For a design with new materials or geometries (e.g. placement of the heater on a membrane) statements about feasibility and necessary geometries must be made. With our program the heat conducting layers can be designed to fit the following design rules:

- The low-pass filter between heater and ink must have a high cutoff frequency to guarantee a good thermal contact.
- The low-pass filter between heater and sink must have a defined cutoff frequency to guarantee a well-timed delay for removal of the residual heat after vaporization. This item has most importance at resolutions of 600dpi and more, because the higher drop rates, reachable at high resolutions by the faster capillary refill, require faster heat removal.
- The design of the entire structure must be sized for sufficient heat dissipation at maximum drop rate.

Item 2: Ink Flow

A model that describes the mechanisms of flow in interaction with a vapor bubble is very useful, but it cannot alone answer some basic questions, like:

- How should a throttle be shortened for constant drop mass if you reduce its cross-sectional area? What is the influence on the refill time?
- How can the heater area be adapted for constant drop velocity if you scale down the design? How does efficiency decrease with scaling?

The main problem is that every parameter change effects the working point of the system. Hence the need for an optimization framework that allows the fixing of some parameters of the working point.

Item 3: Mechanical Design

Not every micromechanical structure is suitable for bubble jet design. For example, thin membranes might be too flexible for a sufficient crosstalk suppression.

The simulation program simulates one active channel with a vapor bubble, one passive indicating channel and a common separating structure (as shown in Figure 1). With good predictions for crosstalk it is possible to design structures with opportunate stiffness.

Results

The following results are answers to typical questions which arise in the bubble-jet design. All samples assume a 300dpi edge-shooter design.

Question 1: Variation of Drop Mass

For a given device, the controllability of the drop size through variation of heating power depends on the length of the nozzle, measured from the vapor bubble to the outlet opening, because the ink in the nozzle works as an energy storage for the power peak in the first few microseconds of the bubble's lifetime.

The simulation results in the following two diagrams show the relation between heater current and drop size/velocity for designs with short (50μm), medium (150μm) and long (300μm) nozzles. The heater area of each type is adjusted to achieve the same drop velocity at the nominal heater current (100% point).

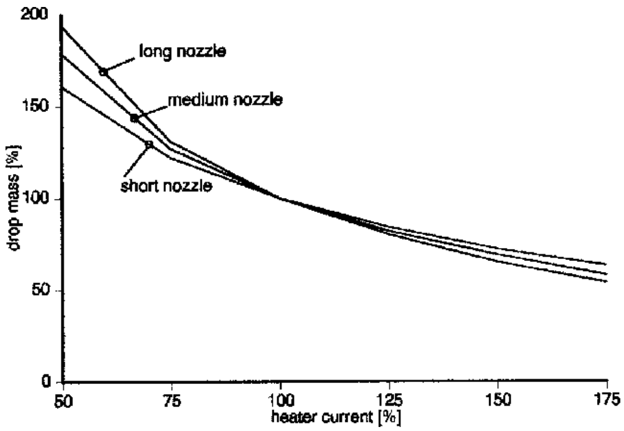

Figure 7. Drop mass variability by heating power for devices with different nozzle lengths

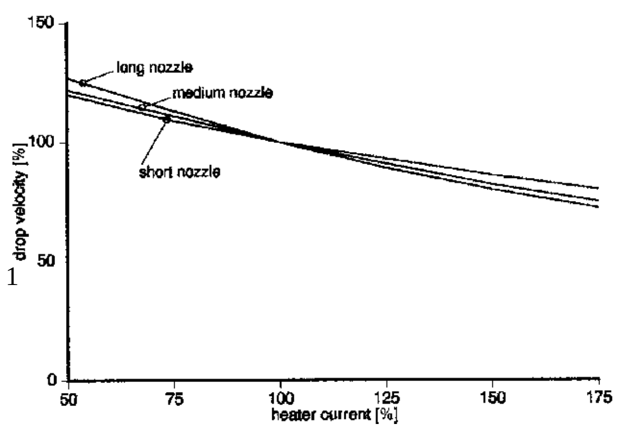

Figure 8. Influence of drop mass variation on drop velocity

Figure 7 and 8 show that a long nozzle is most suitable to control drop size, but with the undesired side effect that the drop velocity also changes.

Question 2: Nozzle Design

Efficiency of the device (drop energy divided by heating pulse energy) is also important. Designs with a different nozzle/throttle length ratio and the same cross-section of nozzle and throttle were simulated. The heater area was adjusted for constant velocity to make the results comparable at the same working point.

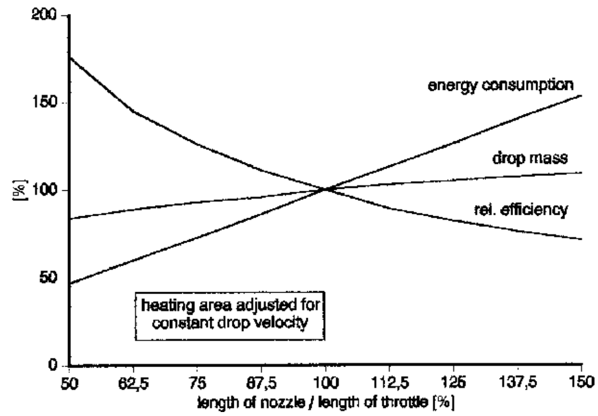

Figure 9. Influence of the nozzle length on typical characteristics of a bubble-jet device

The energy consumption is approximately proportional to the nozzle length. The drop mass stays nearly constant and so efficiency decreases with longer nozzles.

In conclusion, a longer nozzle gives a slightly better control on drop size but is less efficient.

Question 3: Throttle Design

For the design of a throttle one can choose between a long wide or a short narrow geometry. In this experiment the cross-section area of the throttle was changed while its length was adjusted for constant drop mass. Figure 10 shows the influence of the throttle variation on refill time and drop velocity.

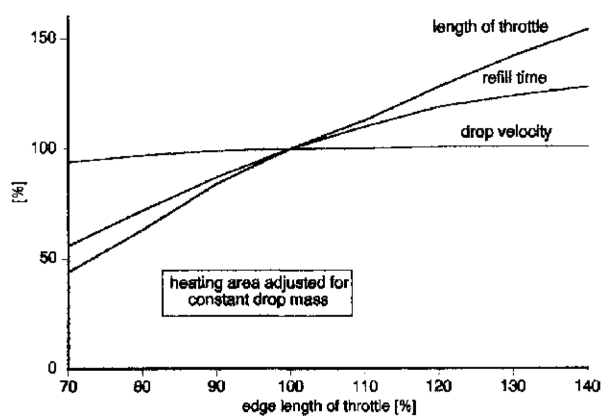

Figure 10. Short throttles guarantee a short refill time without negative side-effects

Question 4: Increasing of Resolution

The first step to increase the resolution of a bubble-jet device would be to scale down the design. Figure 11 shows how, scaling down the size from a typical 300dpi-design up to 1200dpi, drop mass, refill time, energy consumption and efficiency change.

Notes: The heater area has been adjusted for constant drop velocity; energy consumption is proportional to the heater area at constant heating power per unit area;

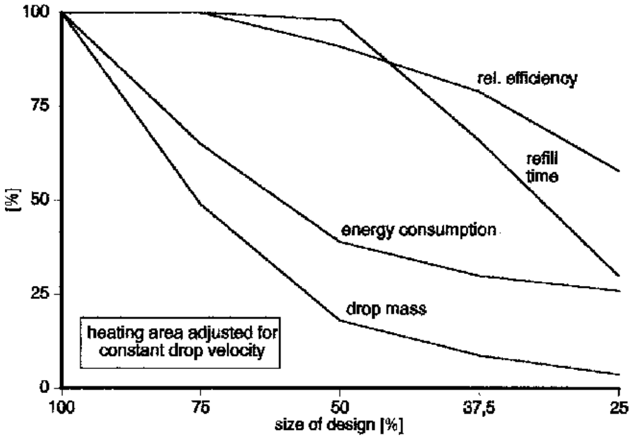

Figure 11. Behavior of a bubble-jet device scaled down from 300dpi to 1200dpi

Computation Time

Each simulation run takes 5 to 10 minutes of calculation time on a PC 486-50. Each optimization run may require 3 to 100 simulation steps. Thus in a time that is very short relative to the production time, the design of a bubble-jet device can be computed and optimized.

Conclusion

The results have already been used for a bubble-jet redesign and the simulation results are in good agreement with the values of the fabricated samples. Drop speed, velocity, and refill time are predicted with an accuracy of 20%.

An additional framework makes it possible to explore the multi-dimensional space of the geometrical characteristics of a bubble-jet device.

References

1. W. Runge, *Berechnungsmodell thermischer Tintenschreibwerke.* Düsseldorf: VDI-Verlag, 1993.
2. W. Runge, Nucleation In Thermal Ink-Jet Printers. *Proc. 8th Int Cong. Adv. Non-impact Printing Techn.*, Williamsburg, Virginia, 1992.
3. E. Truckenbrodt, *Fluidmechanik.* Berlin: Springier, 1980.
4. A. Asai, T. Hara, I. Endo. One-Dimensional Model of Bubble Growth and Liquid Few in Bubble Jet Printers. *Jap. J. Appl. Phys.* **26** (1987).
5. H.-D. Penningsfeld, *Modell der Formung schnell fliegender Mikrotropfen durch Druckwellen an Düsen.* Ph.D. Thesis. Munich, Germany, 1987.